NATIONAL ADVISORY COMMITTEE FOR AERONAUTICS

TECHNICAL NOTE 2909

STUDY OF SECONDARY-FLOW PATTERNS IN AN ANNULAR CASCADE OF TURBINE NOZZLE BLADES WITH VORTEX DESIGN

By Harold E. Rohlik, Hubert W. Allen
and Howard Z. Herzig

Lewis Flight Propulsion Laboratory
Cleveland, Ohio

Washington
February 1953

NATIONAL ADVISORY COMMITTEE FOR AERONAUTICS

TECHNICAL NOTE 2909

STUDY OF SECONDARY-FLOW PATTERNS IN AN ANNULAR CASCADE OF TURBINE NOZZLE BLADES WITH VORTEX DESIGN

By Harold E. Rohlik, Hubert W. Allen, and Howard Z. Herzig

SUMMARY

In order to increase understanding of the origin of losses in a turbine, the secondary-flow components in the boundary layers and the blade wakes of an annular cascade of turbine nozzle blades (vortex design) were investigated. A detailed study was made of the total-pressure contours and, particularly, of the inner-wall loss cores downstream of the blades.

The inner-wall loss core associated with a blade of the turbine-nozzle cascade is largely the accumulation of low-momentum fluids originating elsewhere in the cascade. This accumulation is effected by the secondary-flow mechanism which acts to transport the low-momentum fluids across the channels on the walls and radially in the blade wakes and boundary layers. The patterns of secondary flow were determined by use of hydrogen sulfide traces, paint, flow fences, and total-pressure surveys.

At one flow condition investigated, the radial transport of low-momentum fluid in the blade wake and on the suction surface near the trailing edge accounted for approximately 65 percent of the loss core; about 30 percent resulted from flow in the thickened boundary layer on the suction surface and about 35 percent from flow in the blade wake.

INTRODUCTION

Whenever turning of a fluid is accomplished, as by a cascade, a balance is established between static-pressure gradients and centrifugal forces in that fluid. In an annular cascade where three-dimensional turning is involved, there exist both radial and circumferential static-pressure gradients. These pressure gradients, developed in the main stream, are imposed upon the boundary layers of low-momentum fluid on the walls and on the blades of the cascade. Turning in the boundary layers equal to the free-stream turning would not be sufficient to maintain

balance between the pressure gradients and the centrifugal forces. Thus, more than free-stream turning of the low-momentum boundary-layer fluids results. The deviations in flow direction of the boundary layer from the free-stream flow directions result from the so-called secondary flows. Secondary flows inevitably result from the turning of fluids having boundary layers; in annular cascades, a system of three-dimensional secondary flows must always be established.

Secondary flows in turbine nozzle blades affect cascade performance by influencing the distribution of flow angle and total pressure at the cascade exit. Knowledge of the magnitudes and the flow paths of the various secondary-flow components is necessary in determining the extent of this influence on cascade performance.

Indications of the location and direction of secondary-flow components in a cascade of turbine nozzle blades are presented in reference 1. The angle gradients associated with the secondary-flow systems and their effect on rotor-blade angles of attack are also discussed in reference 1.

The investigation described in this report was conducted at the NACA Lewis laboratory in order to increase present understanding of the flow in an accelerating annular cascade by evaluating the secondary-flow components in the boundary layers and blade wakes.

The blades of the cascade described in reference 1 were modified for use in this investigation. The modifications consisted of flow fences and notches in the blade trailing edges intended to interrupt the secondary-flow components in the blade boundary layers and blade wakes. The results of these modifications were investigated by means of detailed total-pressure measurements at the exit of the blade row at average mainstream Mach numbers at the hub of 0.94 and 1.46.

PRELIMINARY CONSIDERATIONS

A picture of the secondary flows in an annular cascade of turbine-nozzle blades of vortex design is presented in reference 1. The present investigation is an extension of the work reported in reference 1; the same test apparatus and instrumentation, which are shown schematically in figure 1, were used. For the convenience of the reader, a brief statement of the findings of reference 1 and some of the figures are presented herein. The investigation of reference 1 was conducted with the free-stream inlet conditions held constant for each of two exit conditions.

For flow condition I (hub Mach number, 0.94), the indications of cross-channel secondary flows (ref. 2) obtained by the use of hydrogen sulfide traces on white lead paint are presented in figure 2. Measurements at the blade exit (fig. 3) showed loss cores at the inner and outer walls of the cascade. No strong indications of radial flow were obtained for condition I.

At flow condition II (hub Mach number, 1.46), similar indications of cross-channel boundary-layer flows were obtained. An examination of the loss cores in the measuring plane at both conditions, figures 3(a) and 3(b), discloses that the loss region measured at the outer wall at the higher Mach number was actually smaller than at the lower Mach number. This result was considered evidence that some of the low-momentum fluid must flow radially toward the inner wall on the blade or in the blade wake.

The results of the use of a free-flowing paint to trace the radial components of flow on the blades and in the blade wakes are shown in figure 4. Narrow bands were painted on the suction surfaces of the blades at three radial locations: near the outer wall, at midspan, and near the inner wall. The radial flow of paint from the outer to the inner wall at condition II (fig. 4) provided further indications of the radial flow from the outer- to the inner-wall regions.

There are, of course, components of radial flow everywhere in the blade boundary layers. In general, these boundary layers in the turbine-nozzle cascade are thin; a typical velocity profile is shown in figure 5(a). The high through-flow velocities which exist in all but very small regions in such thin boundary layers tend to prevent any sizeable transport of material from the tip to the hub. In order for quantities of low-momentum fluid to flow the entire distance from the outer wall to the inner wall, there must exist some sizeable regions, extending from tip to hub in a passage, in which the through-flow velocities are small (fig. 5(b)). This situation occurs in the wake of the blade. It also occurs along the suction surface of the blade, as described in reference 1, where a shock wave across the passage causes a thickening of the blade boundary layer where this shock wave abuts the blade. The conclusion reached after examination of figure 4 is that there is just this sort of radial transport of low-momentum fluid for condition II. Furthermore, this means that some of the loss-core material measured at the inner wall actually originates at the outer wall. Figure 6 shows schematically the paths (indicated in ref. 1) in which the low-momentum fluids are transported toward the inner-wall loss region as a result of the secondary-flow mechanism.

The investigation described in this report was undertaken in an effort to learn more about the origin and the disposition of secondary flows and, in particular, to verify the indications of reference 1 that flow losses which originate at the outer wall comprise a portion of the losses measured at the inner wall. The blades were modified in an effort to interrupt the secondary flows in such a manner as to enable evaluating the various components of the secondary flows. The major part of the investigation was concerned with the effects of various modifications on the radial transport of low-momentum fluid to the inner-wall region. Resultant changes in the size of the loss core at the inner wall were used to evaluate the results.

APPARATUS

A schematic view of the test rig is presented in figure 1. A complete description of the mechanical details of the rig and of the blades, which were designed for vortex flow, is presented in reference 1.

The modifications shown in figure 7 were adopted in the attempt to separate and to evaluate the various components of secondary flow. These are:

(1) The flow fence (fig. 7(a)) at blade mean radius for interrupting radial flows in the wake of the blade and on the suction surface near the trailing edge

(2) The modified flow fence for interrupting radial flows in the wake, but not in the thickened boundary layer (fig. 7(b))

(3) A 3/16-inch notch in the blade trailing edge (fig. 7(c))

(4) A 3/8-inch notch in the blade trailing edge (fig. 7(d)).

Total-pressure measurements in the measuring plane were made with the three-dimensional probe and the boundary-layer total-pressure probe described in reference 1. In addition, static pressures were measured by eight closely spaced static-pressure taps in either wall at the measuring plane.

PROCEDURE

Effects of the various modifications on loss distribution in the measuring plane were investigated at two exit flow conditions. At condition I, the hub Mach number in the measuring plane was 0.94, and at condition II, it was 1.46. The inlet flow conditions were the same for both exit flow conditions; that is, an inlet total pressure of 26.50 inches of mercury absolute, an inlet total temperature of 553° R, and the inlet pressure distribution shown in figure 8.

Circumferential surveys of total pressure were made at several radial positions in the measuring plane. These surveys, as well as points in each survey path, were spaced to give a detailed picture of each loss region. This spacing varied from one modification to the next because of the differences in loss distribution. An example of the distribution of survey points is shown in figure 9, where the locations of the total-pressure measurement points are plotted for modification I at condition II.

Static-pressure values for points in the stream were calculated from pressure measurements made with wall static taps. It was assumed in this

calculation that the static pressure varied linearly from inner to outer wall along lines in the radial measuring plane which were approximately parallel to the blade wakes shown in figure 3.

Results of the investigation are described in terms of local loss, where this loss is defined as

$$\text{Loss} = 1 - \frac{V_a^2}{V_i^2} = \frac{\left(\frac{p_2}{P_2}\right)^{\frac{\gamma-1}{\gamma}} - \left(\frac{p_2}{P_1}\right)^{\frac{\gamma-1}{\gamma}}}{1 - \left(\frac{p_2}{P_1}\right)^{\frac{\gamma-1}{\gamma}}}$$

where

V_a actual velocity as determined from exit static pressure and indicated total pressure at exit

V_i ideal velocity as determined from exit static pressure and reference inlet total pressure

p_2 exit static pressure

P_2 indicated exit total pressure

γ ratio of specific heats

P_1 reference inlet total pressure

The error involved in the losses calculated from pressure measurements made at condition I is believed to be negligible because of the Mach number level. At condition II, however, the total pressures indicated by the probes are low because of the shock losses associated with the probes. These shock losses varied with position in the measuring plane because of the variation in Mach number as well as the proximity to the loss regions. Near the hub boundary layer, for example, interaction of the shock wave induced by the probe and the shroud boundary layer produced a thickened boundary layer which influenced flow just upstream of the probe by causing a series of very weak oblique shocks. This boundary-layer thickening upstream of the incident shock wave is discussed in reference 3, which contains schlieren photographs at several shock strengths and Reynolds numbers. Because the air had thus decelerated through a series of weak oblique shocks rather than one normal shock upstream of

the probe, the indicated total pressure was higher than that considered possible for the Mach number level and a normal shock. Accurate correction for the error induced by the presence of the probes at each measuring point in the stream is therefore extremely difficult.

The static pressures in the stream when the probes were withdrawn indicated that the maximum normal-shock-loss correction necessary anywhere in the measuring plane was slightly greater than 5 percent. The 5-percent loss contours in figure 12 clearly define the loss regions existent with each modification at condition II and separate the viscous-loss areas from the areas in which this variable probe loss is the only loss. In evaluating the effects of the modifications, then, only the areas within the 5 percent contours were considered; this was done simply by assuming that all losses of 5 percent or less were equal to zero.

RESULTS AND DISCUSSION

In order to establish the reasons for using the changes in size of the inner-wall loss cores as criteria for evaluating the effectiveness of the modifications, the following general discussion of the results is presented.

In general, it was observed that the sheet-metal fences on the blades were effective in blocking the radial flows. (The criterion applied was the effectiveness in reducing the accumulation of low-momentum fluid at the inner wall.) Because the fences increased the wetted surface area in the flow passage, the modifications themselves introduced some viscous losses.

Separation of these modification-induced losses from the low-momentum fluid interrupted by the modifications is not readily feasible. Accordingly, the changes in size of the inner-wall loss core are used as criteria for evaluating the effectiveness of the modifications and as a basis for interpretation of the results.

As expected, none of the modifications used affected the losses near the outer wall under any condition, being "downstream" of the outer wall with respect to the radial flows.

Condition I

Only modification 1 was used for flow condition I, (hub Mach number, 0.94). By comparing figure 10 with figure 3(a), it can be seen that the flow fences apparently had a negligible effect on the inner-wall loss core. Examination of figure 11 also shows this in terms of the circumferentially averaged loss from the inner wall to the fence. From this

fact, and the knowledge that the flow fences effectively interrupt radial flow in the blade wakes (as will be proved in the results for condition II), it is concluded that there is little or no radial flow in the blade wakes at condition I. The losses which appear at the flow-fence position, approximately 1.1 inches from the inner wall, evidently have been generated by the fences themselves.

During the tests to trace the cross-channel secondary flow on the outer wall, faint indications of hydrogen sulfide flowing radially down the trailing edges were noted. These traces, coupled with the observation that there seems to be no a priori reason for the loss core at the inner wall to be so much larger than at the outer wall for these blades, were considered to indicate radial transport of fluid at condition I. One possibility suggested was that radial flow in sufficient quantities to cause this difference in inner-wall and outer-wall core sizes might occur along the blade suction surface where the paint traces showed some indication of flow separation.

In the investigation at condition I, the results showed that radial transport of low-momentum material from the outer-wall region to the inner-wall region may occur, but there was no evidence of where and how much of it takes place. However, indications were that, if such a radial transport did take place, it occurred chiefly along the suction surface upstream of the flow fence.

Condition II

The existence of radial flows that would enable transport of low-momentum fluids from the outer wall to the inner wall was investigated, and measurements were made of the quantities involved with the cascade at condition II (hub Mach number, 1.46).

Modification 1. - The effectiveness of the flow fence, modification 1, is demonstrated by a comparison of figure 12(a) with figure 3(b). The sharp reduction in size of the inner-wall loss core as a result of the flow fences constitutes proof of radial flow and transport of low-momentum fluids from the outer wall to the inner wall. By integration it was determined that approximately 65 percent of the losses which appear in the inner-wall loss-core region (the region from 0.040 to 0.500 in. from the inner wall) come, by means of radial flows in the blade wakes and on that part of the blade surface intercepted by the fence of modification 1, from the neighborhood of the outer wall. These estimates are only qualitative because of the probe errors discussed in the section on procedure but the over-all picture is unmistakable. The circumferentially averaged loss, plotted radially over one-half of the blade height in figure 13, shows the change in loss distribution effected at various radial positions by the flow fences.

The circumferential location at various radial positions of the wake in figure 3(b) indicates underturning in the region near the hub. Comparison of figure 3(b) with figures 12(a) and 12(b) shows that the blade fences effected a reduction in the underturning in this region as well as a reduction in the size of the loss core. This reduction is evidenced by the shift in circumferential position of the loss region near the inner wall. Evidently, a large part of the underturning in that region of the unmodified cascade is caused by flow blockage due to the accumulation of low-momentum fluid.

Modification 2. - A further refinement of the pattern of distribution of the low-momentum fluid is provided by the flow fence in modification 2, (fig. 12(b)), which by acting upon the flow in the blade wakes only, enables an evaluation of the uninterrupted flow through the thickened boundary-layer region where the shock wave abuts the blade suction surface. Thus, of the low-momentum fluid which accumulates in the loss core at the inner wall, about 30 percent is derived from radial flow through the strip of thickened blade boundary layer and about 35 percent from flow through the blade wake.

It is further shown that, in this particular cascade of nozzle blades, the thickened boundary-layer region is comparable in size to the blade wake. This fact is evident from considerations of the static-pressure gradients and the fluid densities involved, which are not greatly different in the two regions. The quantities of flow through these regions, are therefore established as measures of the comparative sizes of thickened boundary layers and the blade wakes.

Modification 3. - Modification 3, a 3/16-inch notch cut into the trailing edge of the blade (fig. 12(c)), was not deep enough to intersect the thickened boundary-layer strip on the blade (fig. 4). The notch was intended to accomplish the same reduction of the inner-wall loss core as the flow fence by providing a discontinuity in the flow path of low-momentum fluid on the blade trailing edge. It appeared likely, because of the rapid dissipation of the wake downstream of the trailing edge below the notch, that low-momentum fluid flowing from the outer wall would be swept downstream at the blade notch. This modification failed notably to disrupt the blade-wake radial flow. Instead, the blade wake and the attendant radial flows remained attached to the trailing edge. The shift in position of the loss core in figure 12(c)(cf. fig. 3(b)), without appreciable change in size, supports this contention.

From figure 12(c), it can be seen further that a few new losses were generated at the trailing-edge discontinuity, 1.1 inches from the hub. It might well have been anticipated that there would be a large flow from the pressure surface to the suction surface along the top edge of the notch in the manner of the tip-clearance losses described in figure 16 of reference 4. In these vortex blades, however, the turning is accomplished

early, and the 3/16-inch notch is in the region where the blades provide mainly guidance and where little further turning of the main flow is involved.

The over-all average loss for modification 3 is thus increased but slightly over that of the unmodified blades.

Modification 4. - Modification 4 consisted of a 3/8-inch notch in the blade trailing edge. In this case the notch, which was deep enough to penetrate the region of the blade where turning is involved, intersected the thickened boundary layer caused by the shock wave in the passage. From the position and size of the losses at 1.1 inches from the inner wall (fig. 12(d)), it is evident that the notch caused underturning. From the large increase in losses at the inner wall, (cf. fig. 12(c)), it must be concluded that large losses are generated by flow from the blade pressure surface to the suction surface at the top of the notch and that these then flow radially to the inner wall.

CONCLUDING REMARKS

Secondary flows have a large effect on the distribution of losses downstream of the blade row. The major result of the secondary-flow mechanism in this investigation was the formation of an inner-wall loss core.

Secondary flows can be intercepted by simple barriers in the flow paths of the low-momentum fluid. Thus, the degree of underturning at the inner wall, caused by blockage which is a result of the loss accumulation by the secondary flow, can be reduced.

The inner-wall loss core is an accumulation of losses which for the most part originate elsewhere in the passage. On paths leading to the loss region in the corner bounded by the blade suction surface and the hub at the blade trailing edge, low-momentum fluid is transported across channels to the suction surfaces in the wall boundary layers, and radially inward in the blade boundary layers and in the blade wakes. At condition II (hub Mach number, 1.46), the radial flows in the blade wake and the thickened boundary layer on the suction surface accounted for approximately 65 percent of the loss core; about 35 percent resulted from flow in the blade wake and about 30 percent from flow in the thickened boundary layer. At condition I (hub Mach number, 0.94), no appreciable radial flow in the blade wakes was observed.

Lewis Flight Propulsion Laboratory
National Advisory Committee for Aeronautics
Cleveland, Ohio, October 31, 1952

REFERENCES

1. Allen, Hubert W., Kofskey, Milton G., and Chamness, Richard E.: Experimental Investigation of Loss in an Annular Cascade of Turbine Nozzle Blades of Free Vortex Design. NACA TN 2871, 1952.

2. Herzig, H. Z., Hansen, A. G., and Costello, G. R.: Visualization of Secondary-Flow Phenomena in Blade Row. NACA RM E52F19, 1952.

3. Barry, F. W., Shapiro, A. H., and Neumann, E. P.: The Interaction of Shock Waves with Boundary Layers on a Flat Surface. Jour. Aero. Sci., vol. 18, no. 4, April 1951.

4. Hansen, A. G., Costello, G. R., and Herzig, H. Z.: Effect of Geometry on the Secondary Flows in Blade Rows. NACA RM E52H26, 1952.

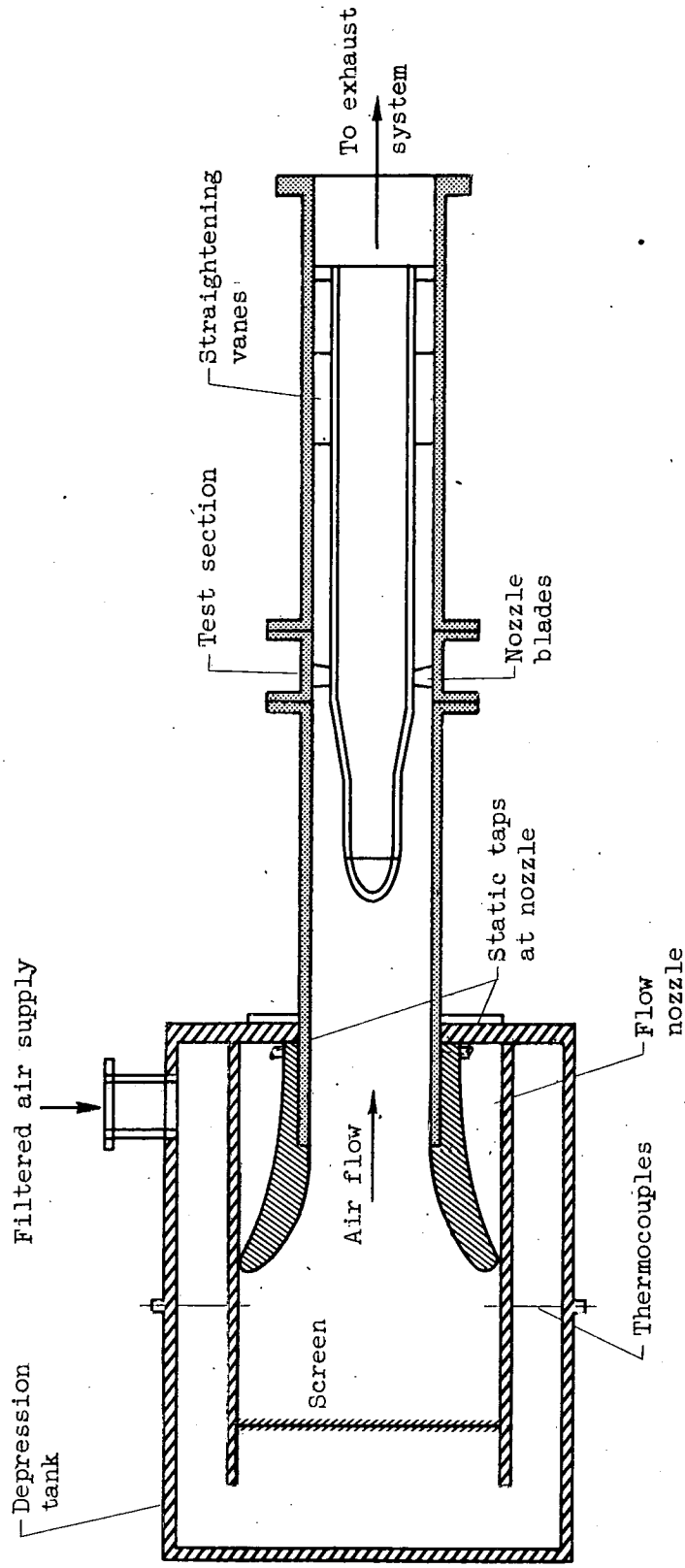

Figure 1. - Schematic view annular nozzle cascade test unit. (Fig. 1 of ref. 1.)

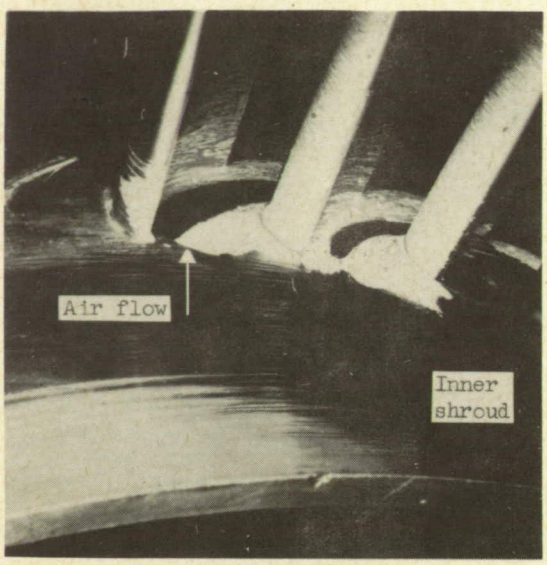

(a) Inner shroud at entrance.

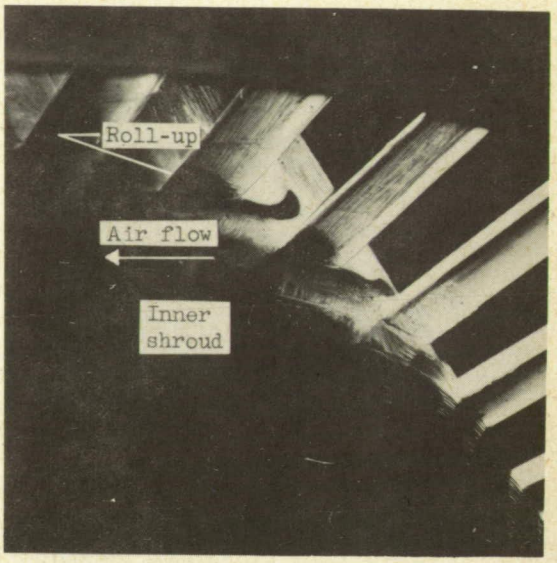

(b) Inner shroud at exit.

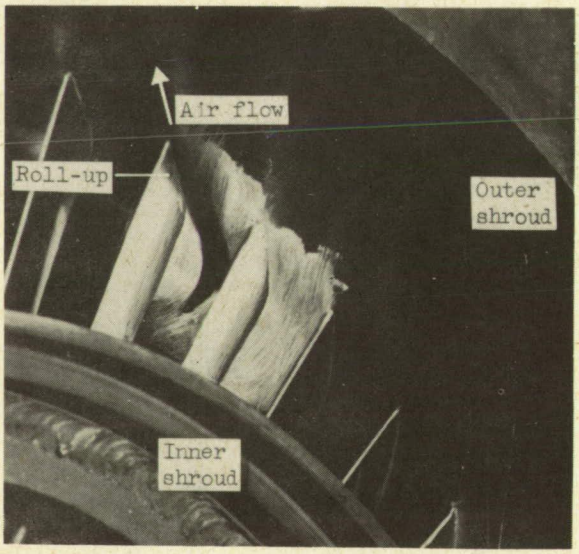

NACA

C-29960

(c) Outer shroud at exit.

Figure 2. - Hydrogen sulfide traces through blade channel. (Fig. 9 of ref. 1.)

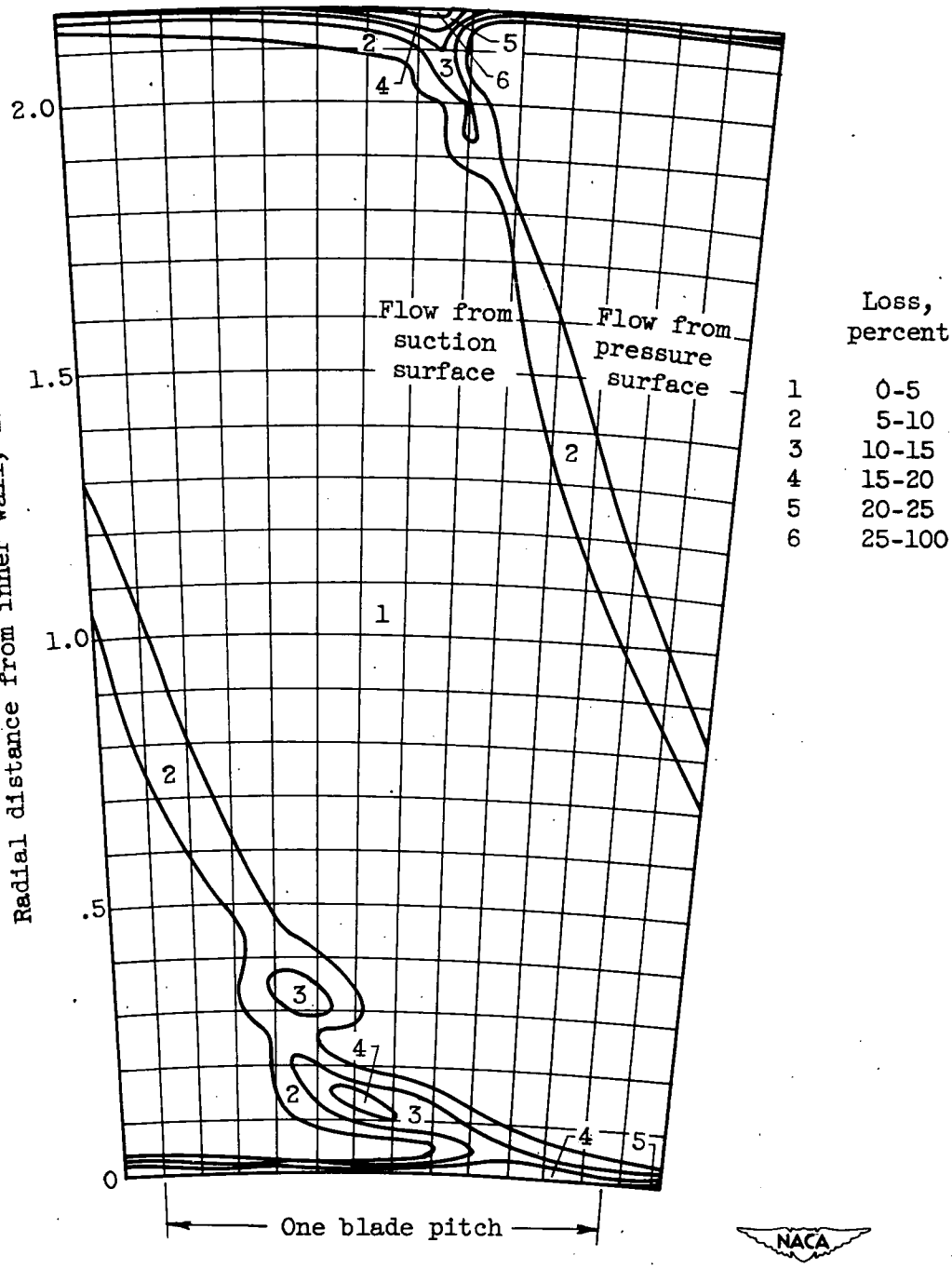

(a) Condition I (hub Mach number, 0.94).

Figure 3. - Contours of energy loss at exit measuring station. (Fig. 5(a) of ref. 1.)

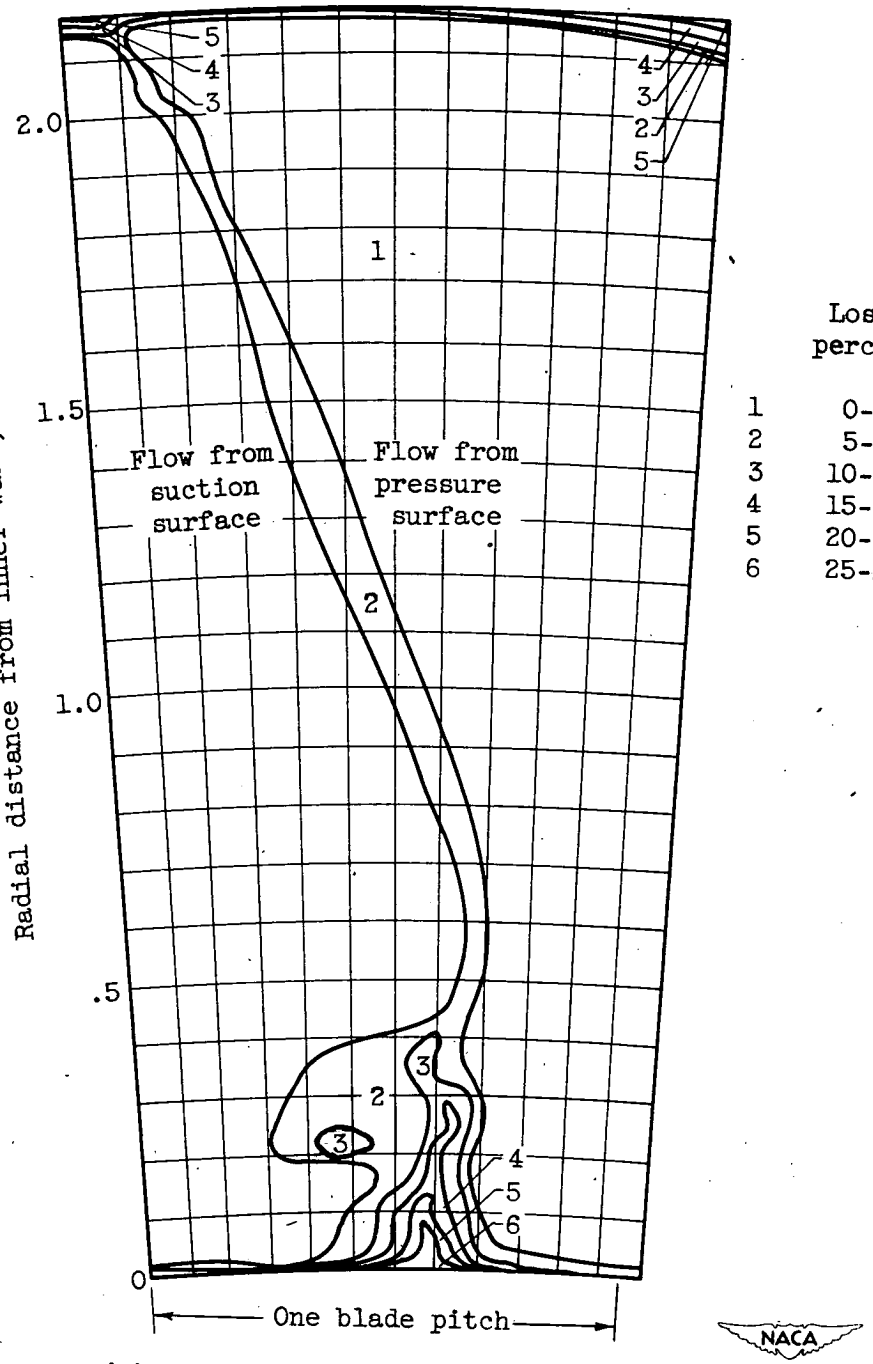

(b) Condition II (hub Mach number, 1.46).

Figure 3. - Concluded. Contours of energy loss at exit measuring station. (Fig. 5(b) of ref. 1.)

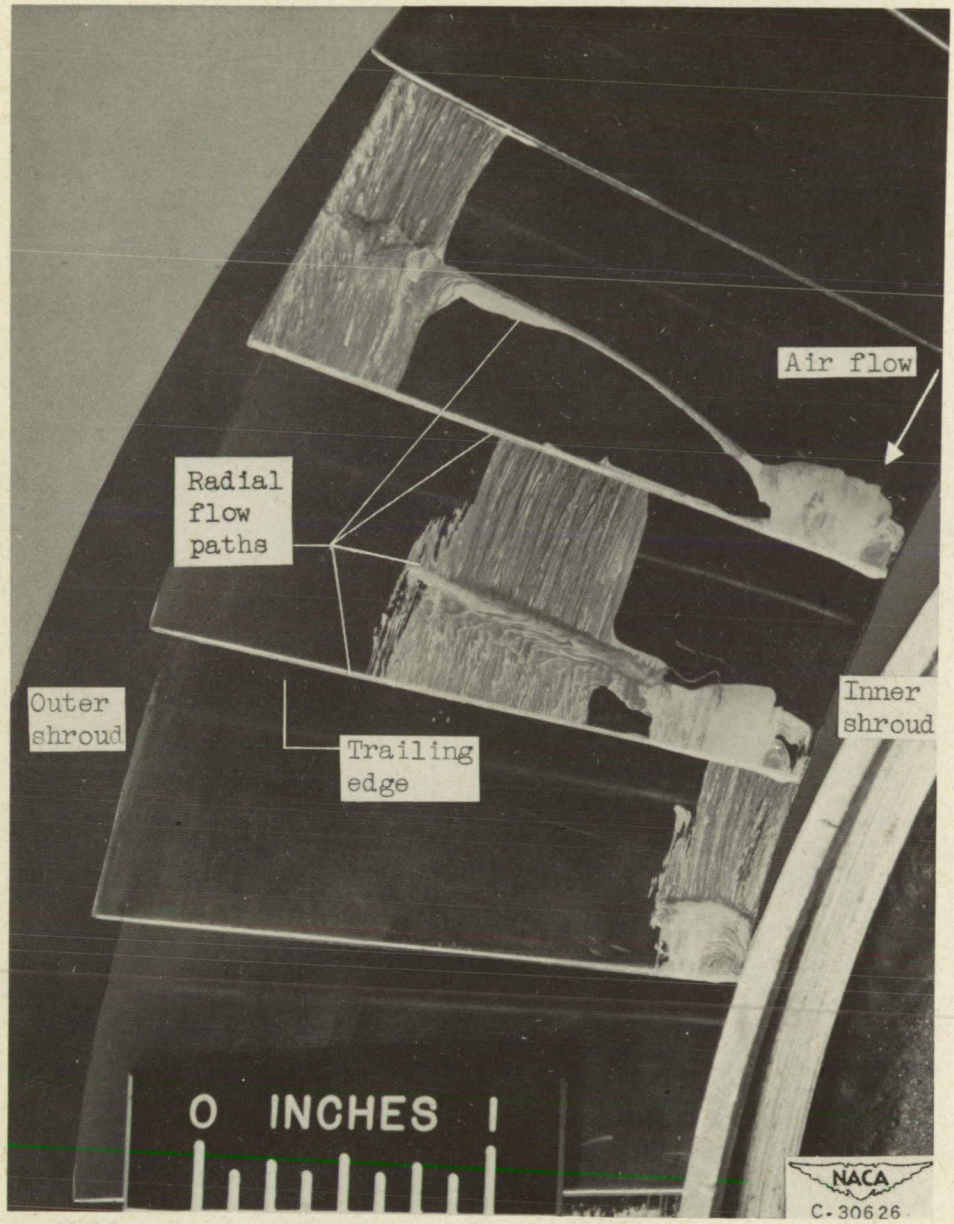

Figure 4. - Paint traces on suction surfaces of blades. Condition II (hub Mach number, 1.46). (Fig. 12 of ref. 1.)

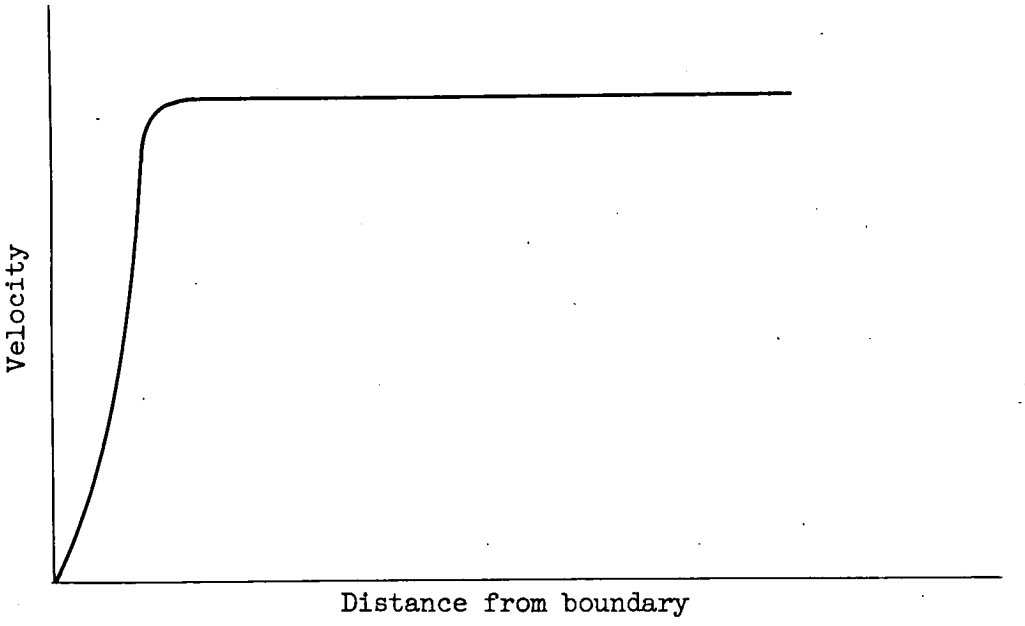

(a) Typical velocity profile for thin boundary layer.

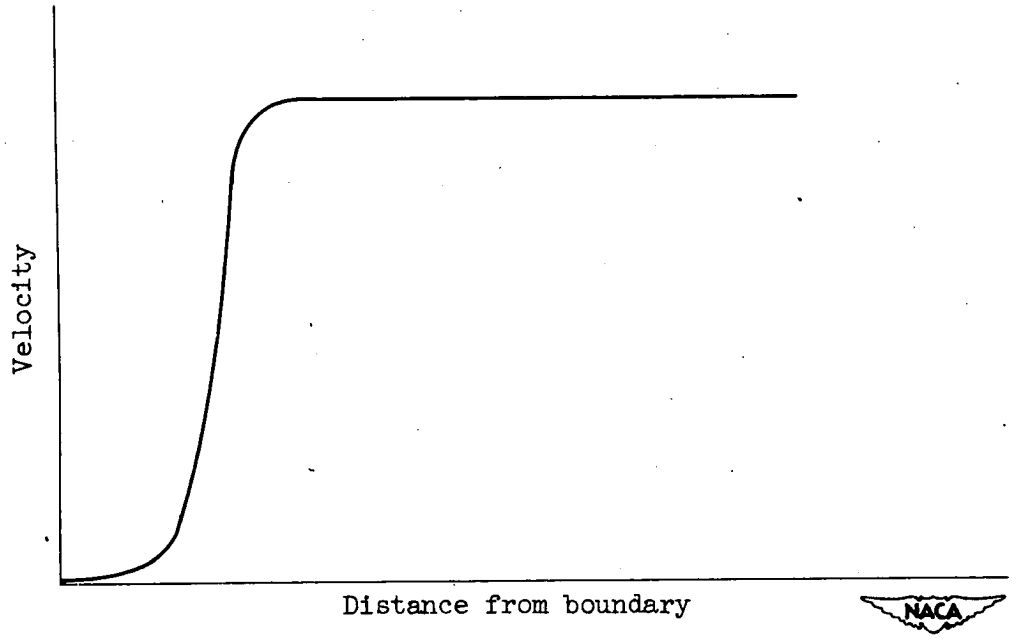

(b) Velocity profile for thickened boundary layer.

Figure 5. - Comparison of velocity profiles for thin and thickened boundary layers.

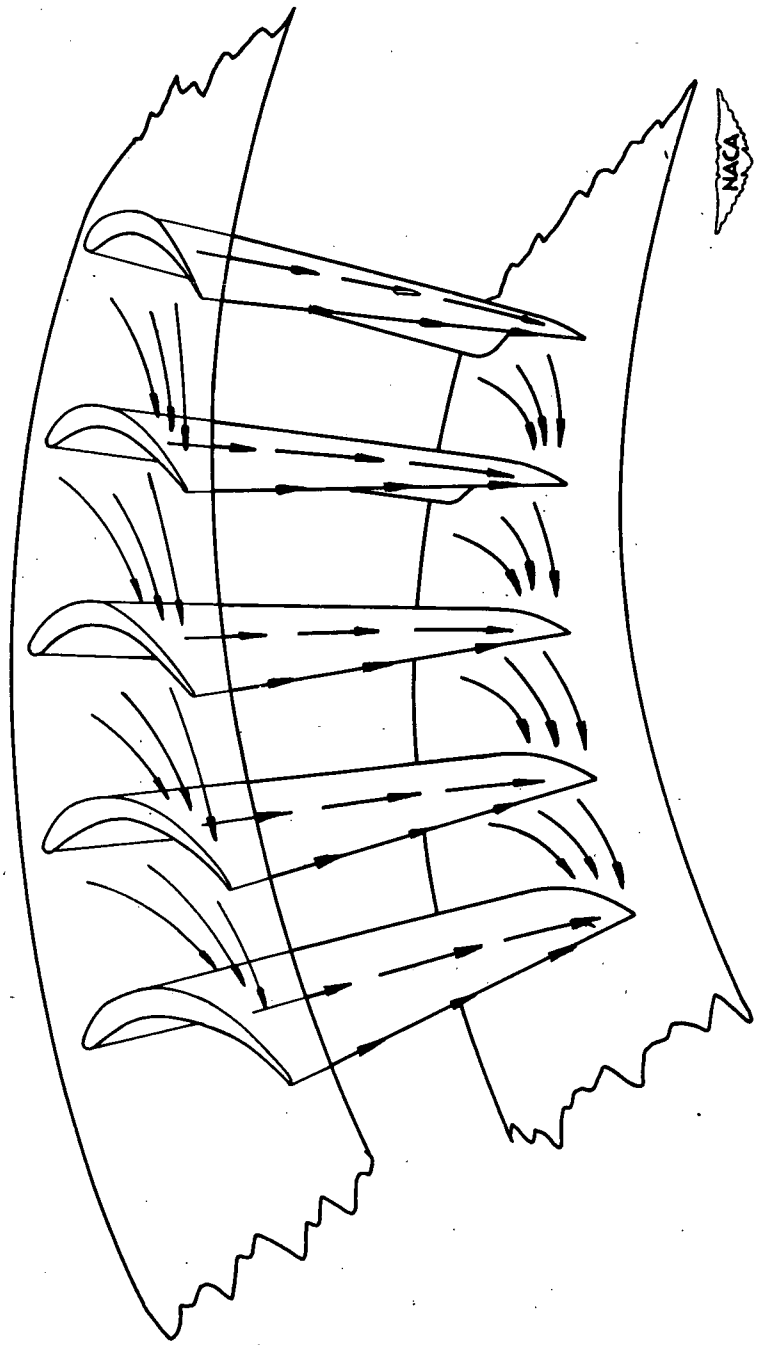

Figure 6. - Secondary flow components at condition II as indicated by paint and hydrogen sulfide traces.

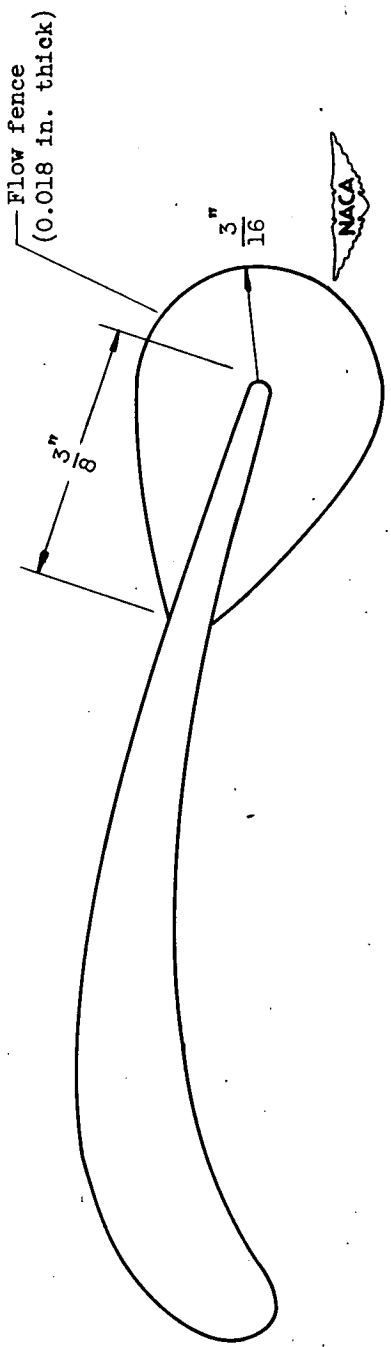

(a) Modification 1.

Figure 7. - Sketches of various modifications.

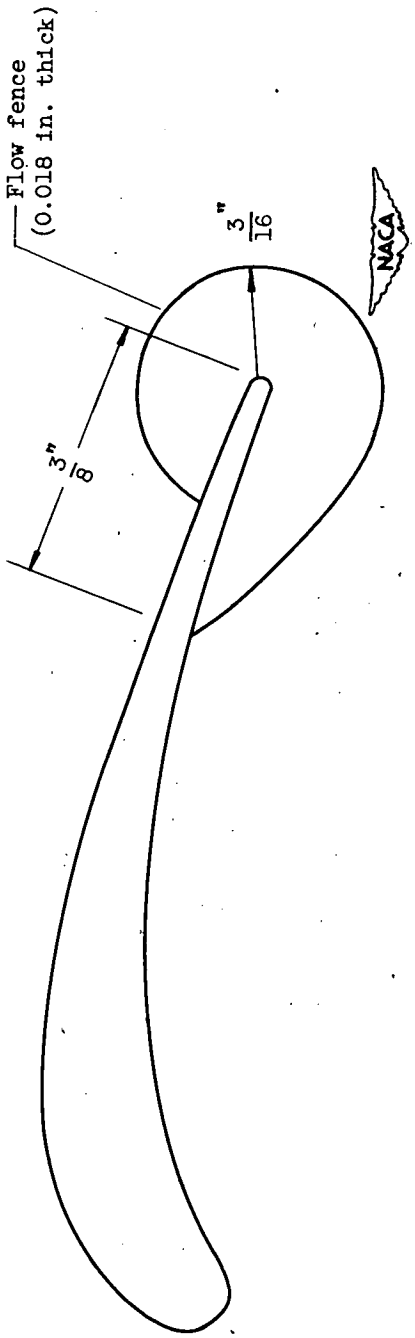

(b) Modification 2.

Figure 7. - Continued. Sketches of various modifications.

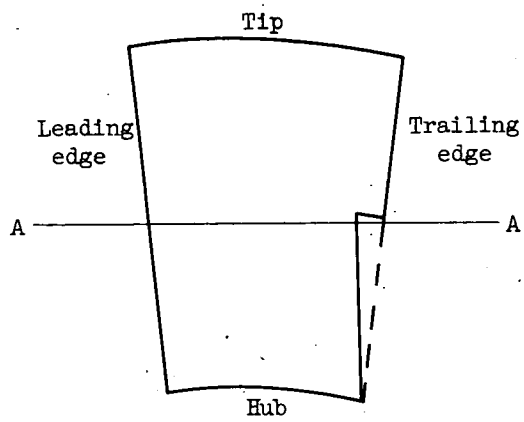

Section A-A

(c) Modification 3.

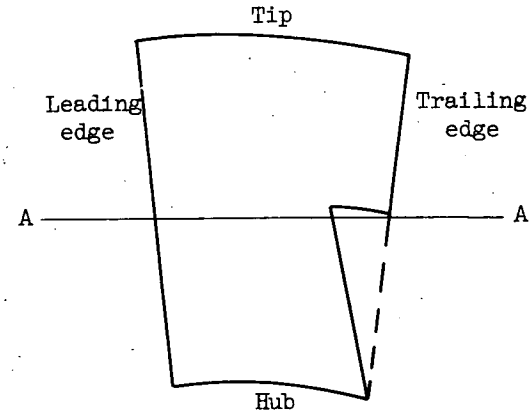

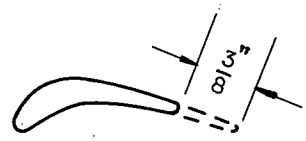

Section A-A

(d) Modification 4.

Figure 7. - Concluded. Sketches of various modifications.

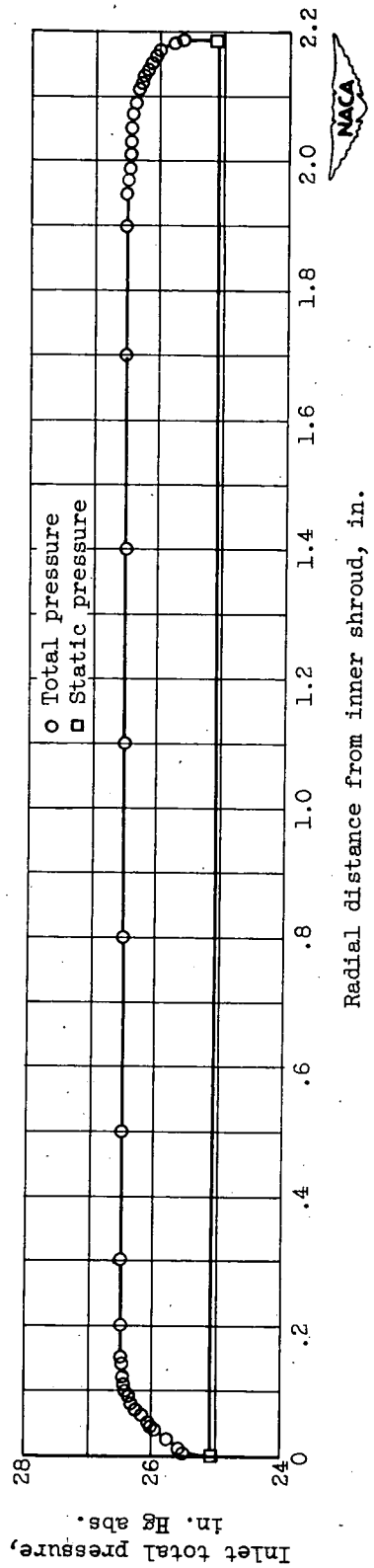

Figure 8. - Inlet-pressure distribution.

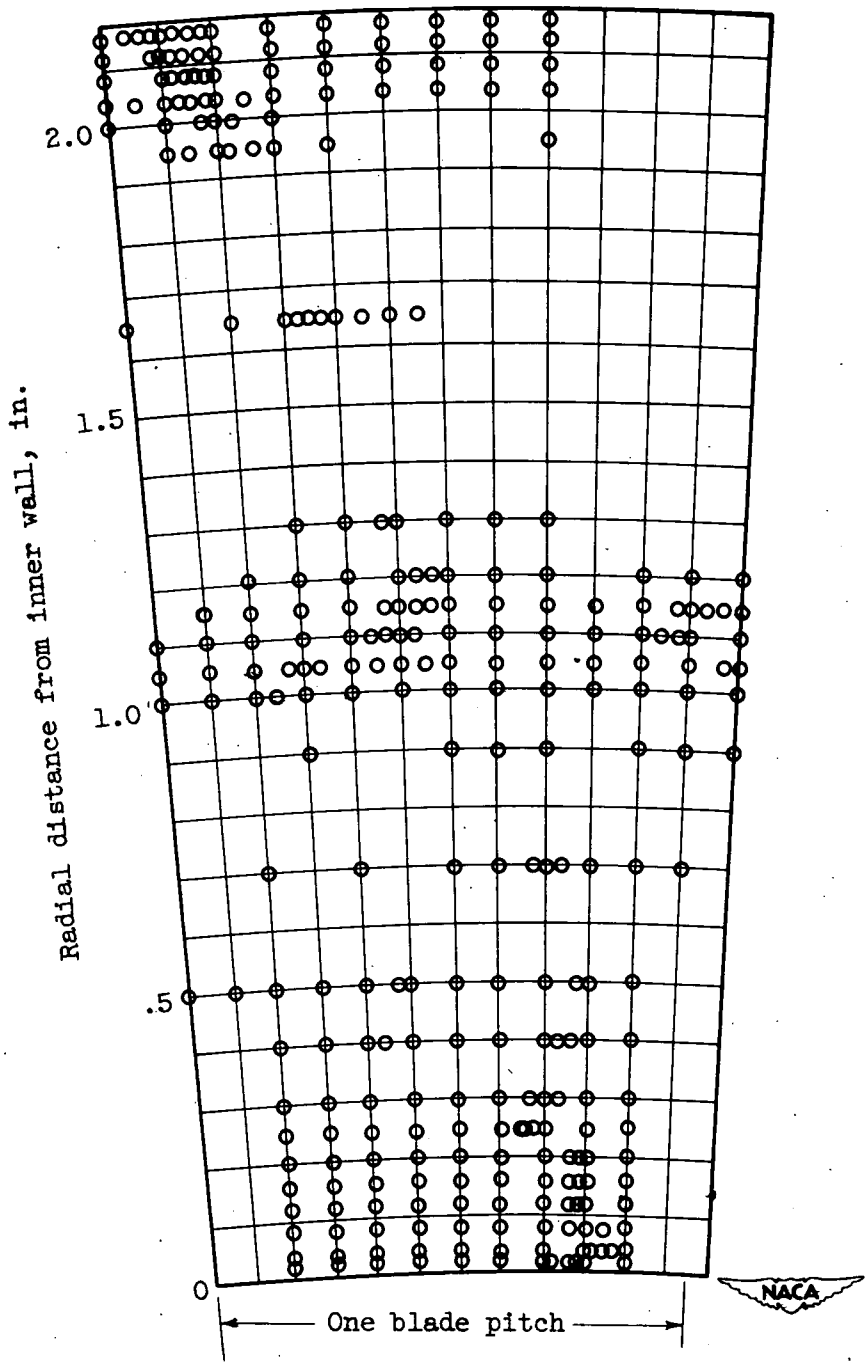

Figure 9. - Total-pressure measurement points for modification 1. Condition II (hub Mach number, 1.46).

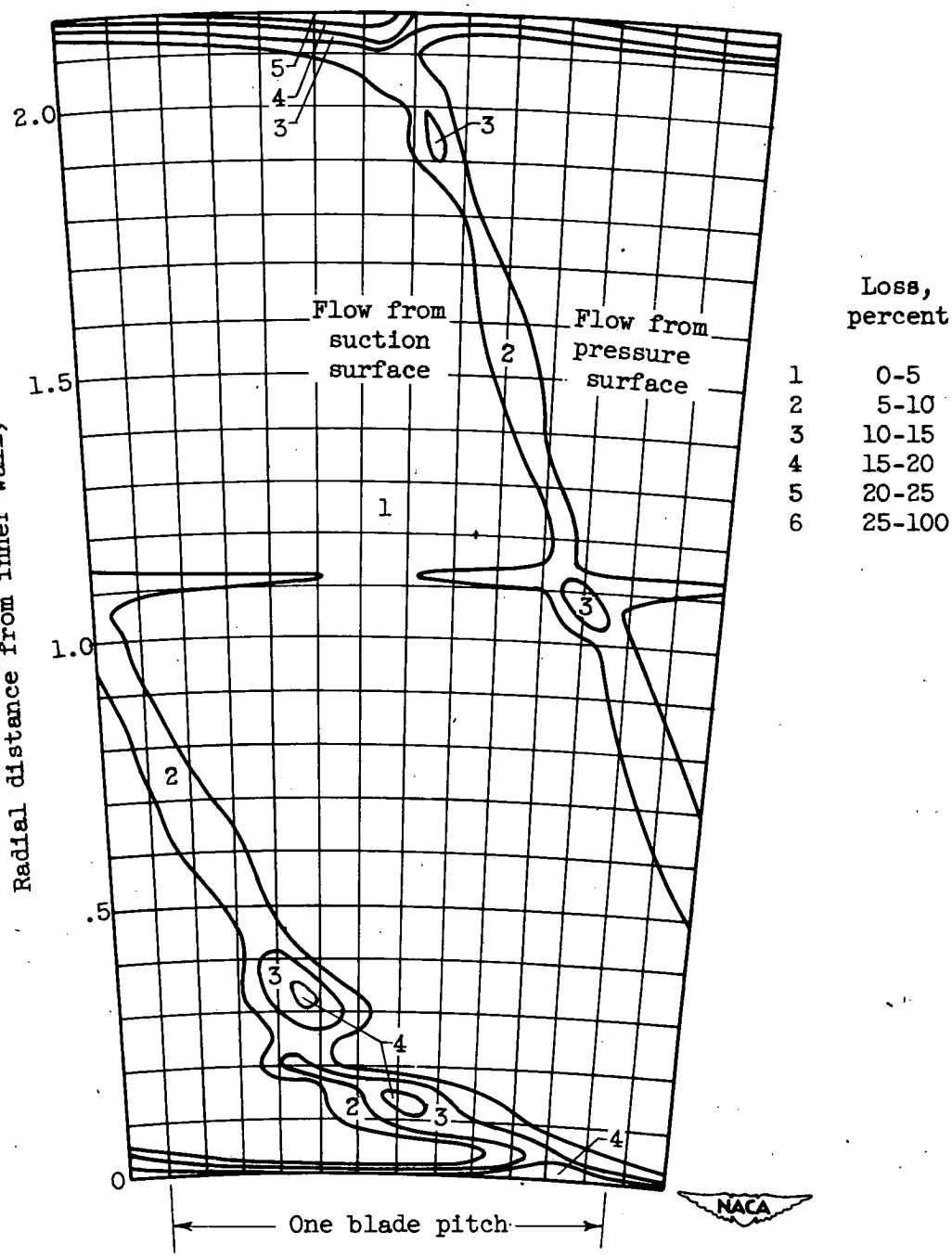

Figure 10. - Contours of energy loss at exit measuring station. Condition I (hub Mach number, 0.94). (Modification 1.)

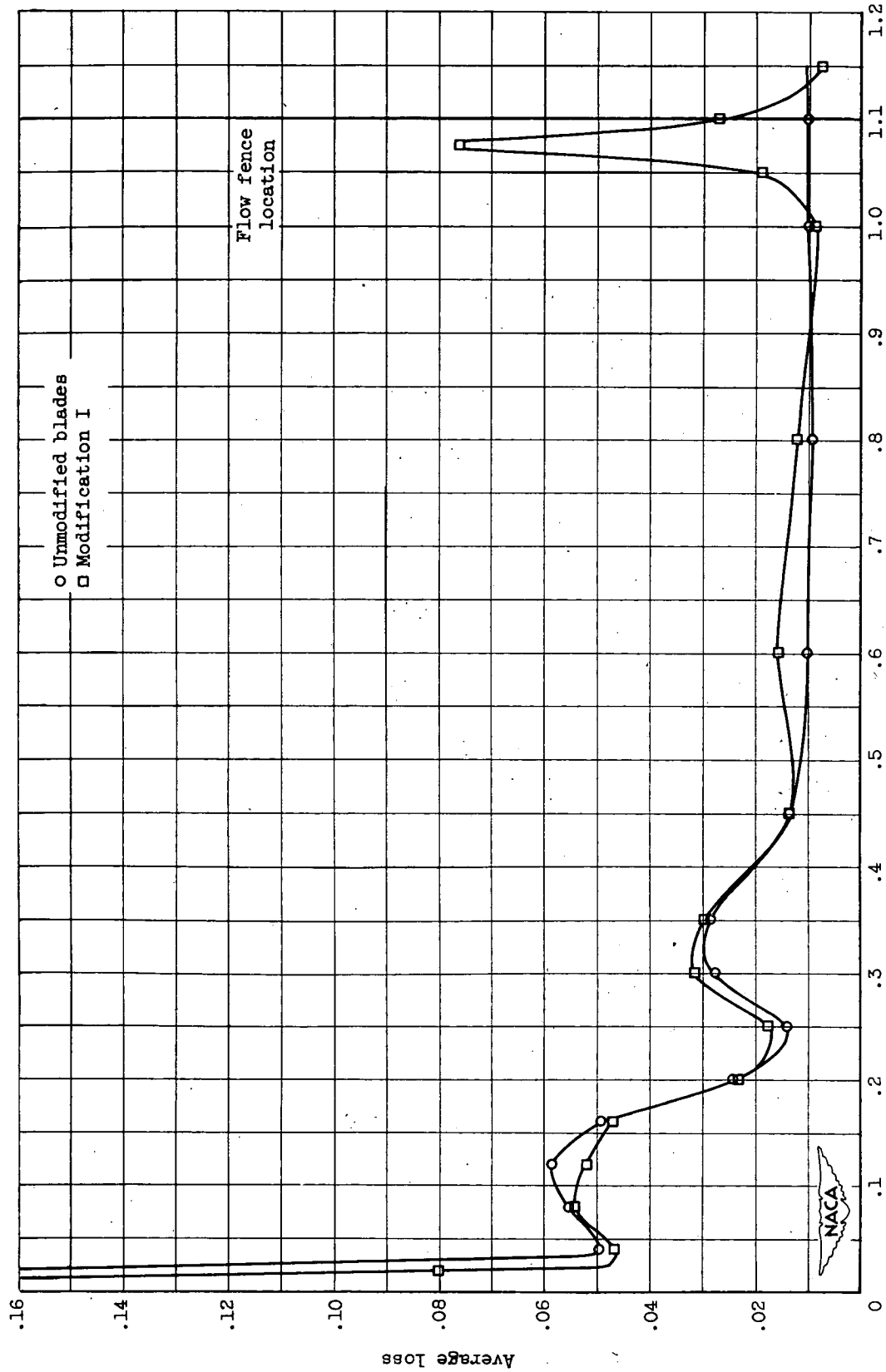

Figure 11. - Circumferentially averaged loss for condition I (hub Mach number, 0.94).

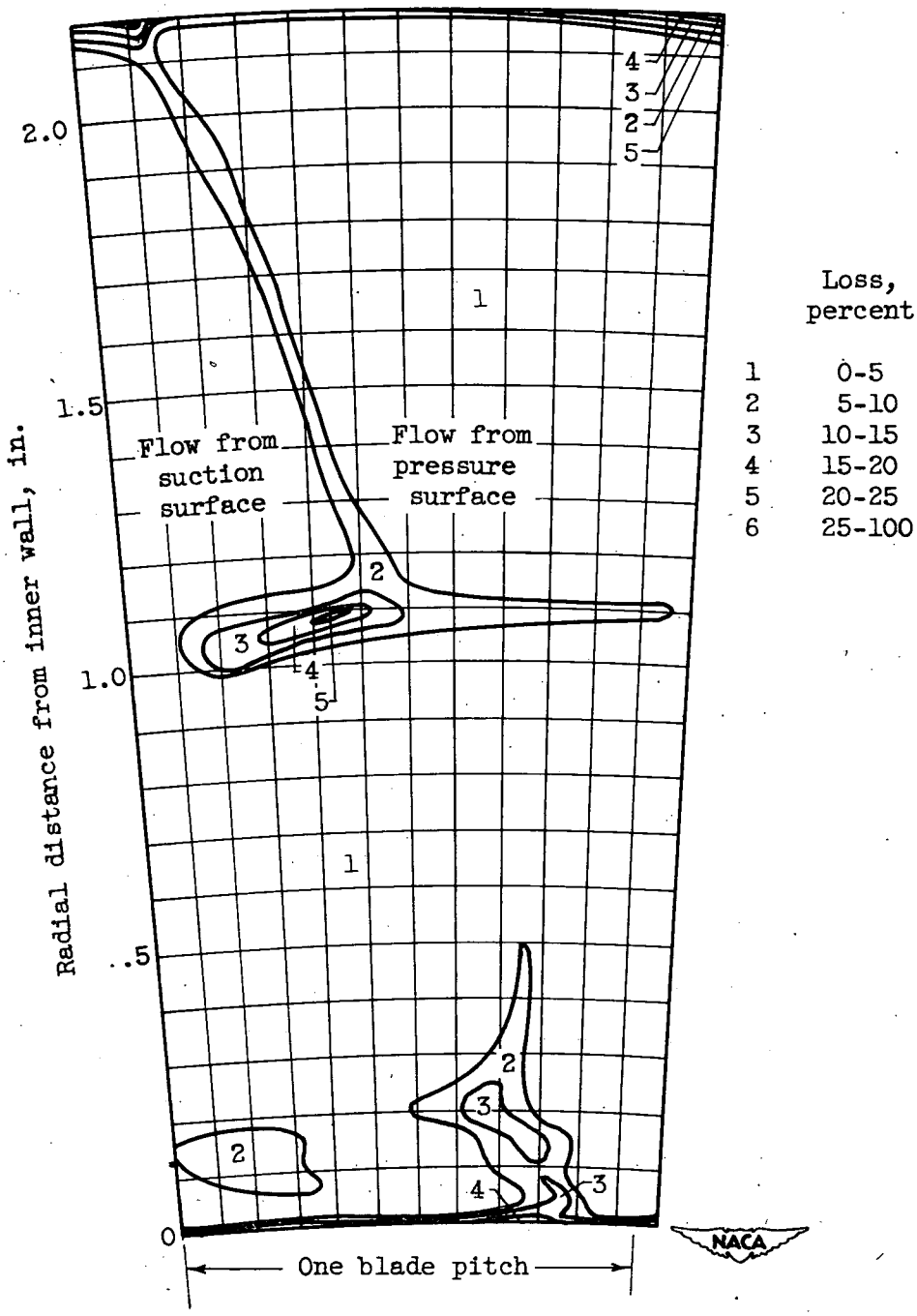

(a) Modification 1.

Figure 12. - Contours of energy loss at exit measuring station. Condition II (hub Mach number, 1.46).

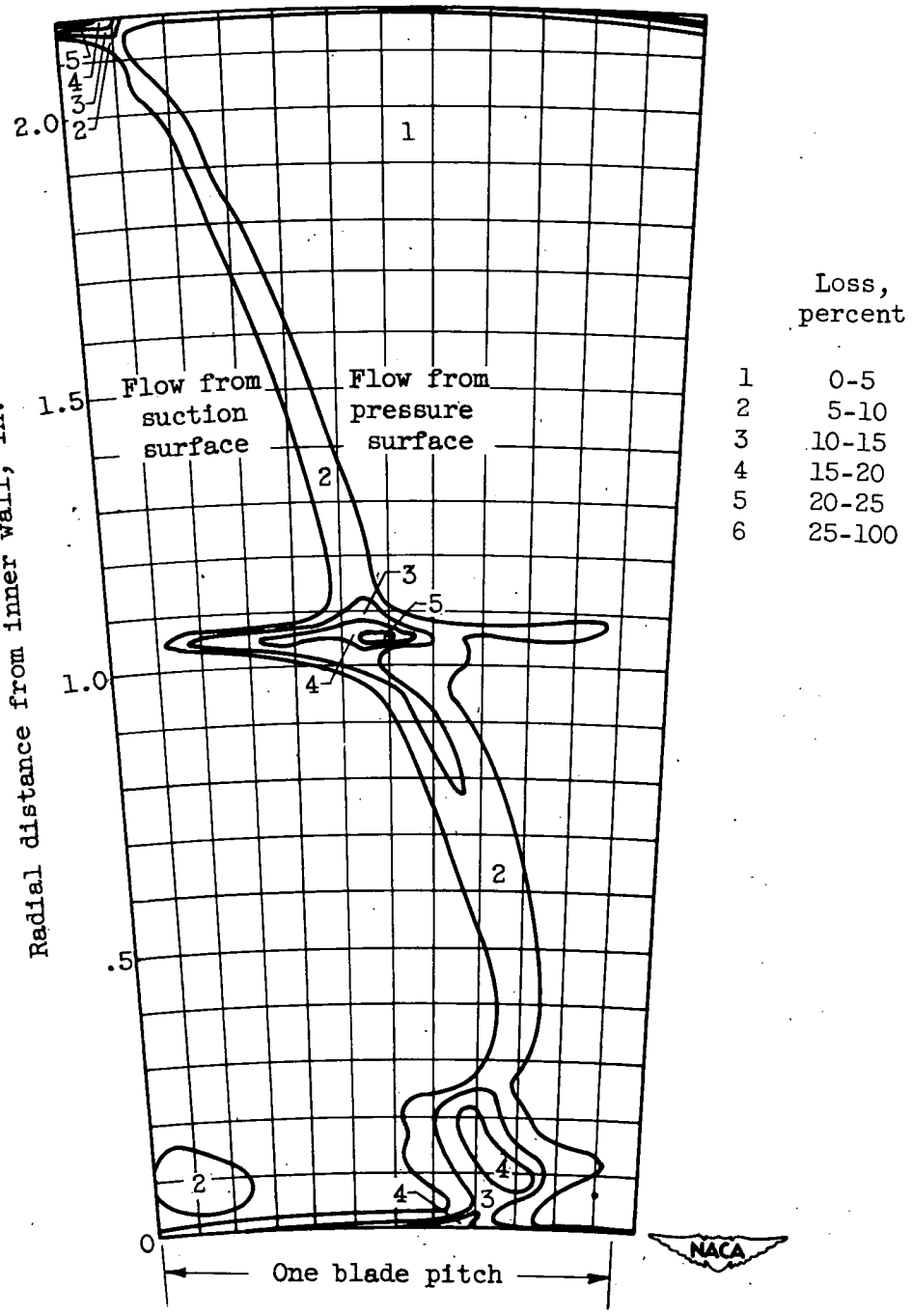

(b) Modification 2.

Figure 12. - Continued. Contours of energy loss at exit measuring station. Condition II (hub Mach number, 1.46).

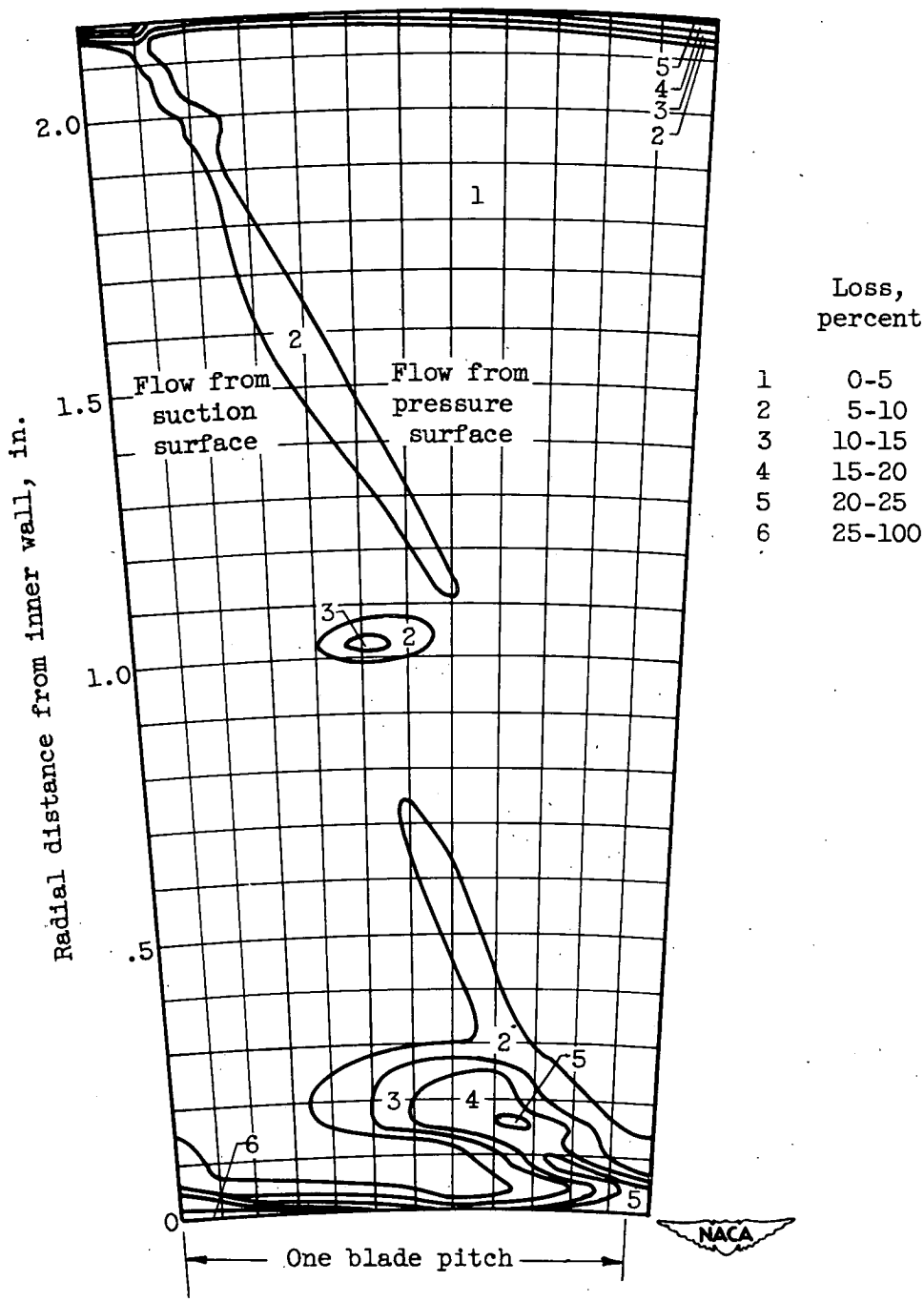

(c) Modification 3.

Figure 12. - Continued. Contours of energy loss at exit measuring station. Condition II (hub Mach number, 1.46).

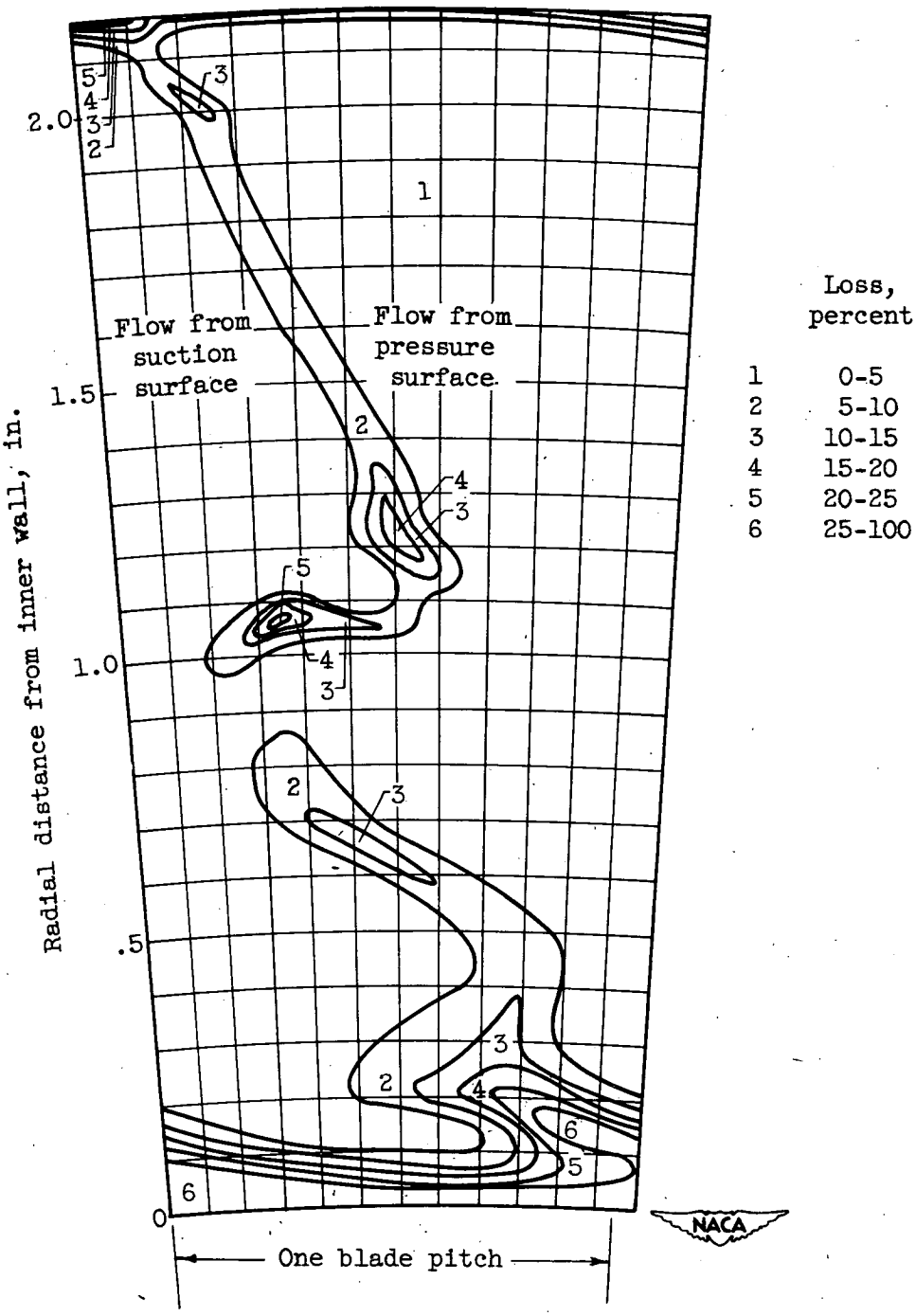

(d) Modification 4.

Figure 12. - Concluded. Contours of energy loss at exit measuring station. Condition II (hub Mach number, 1.46).

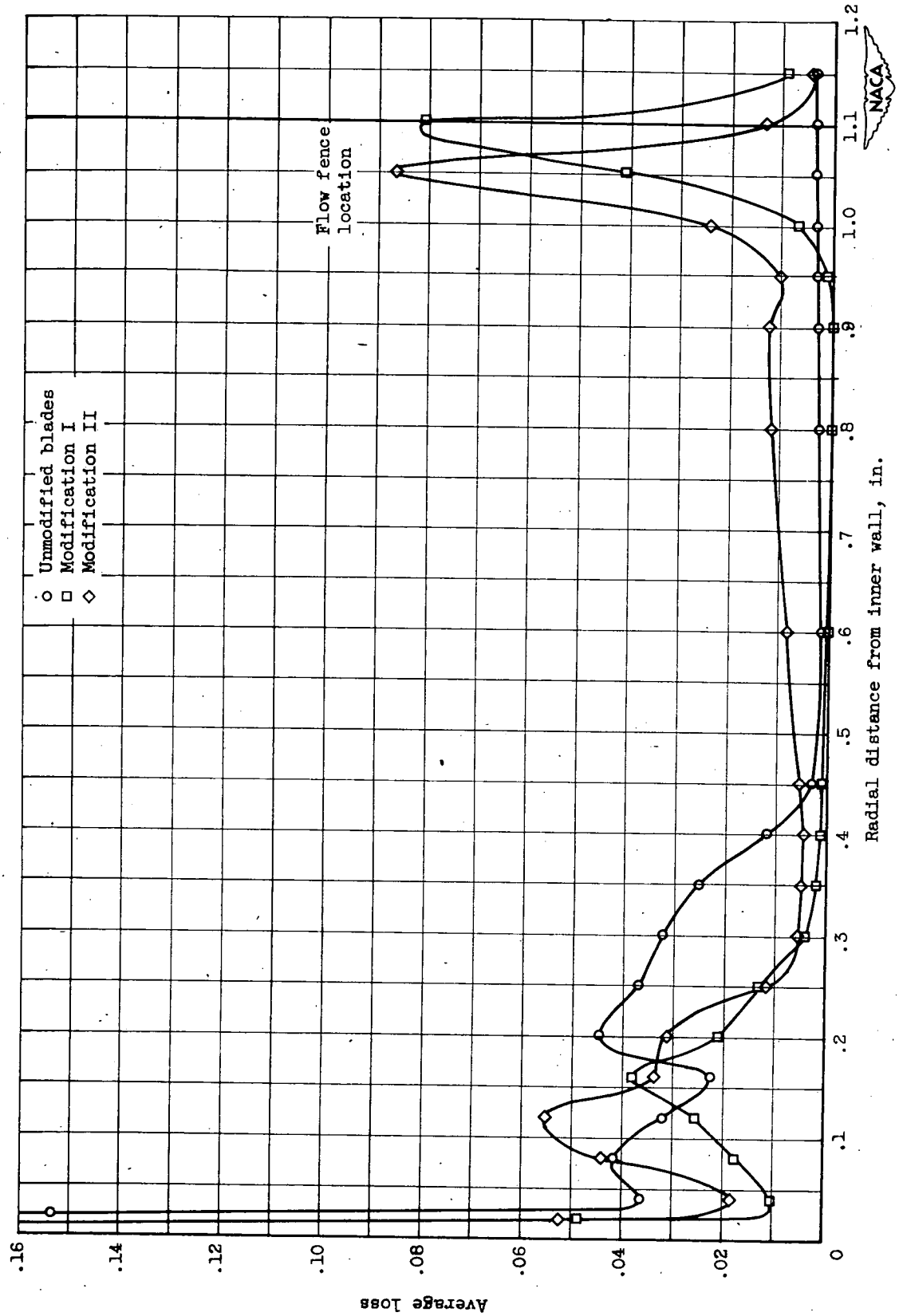

Figure 13. - Circumferentially averaged loss for condition II (hub Mach number, 1.46).